J. Appl. Cryst. (1988). **21**, 79–85

Laboratory EXAFS in a Dispersive Mode

By R. Buschert

Turner Laboratory, Goshen College, Goshen, Indiana 46526, *USA*

M. D. Giardina and A. Merlini

Commission of the European Communities, Joint Research Centre, Ispra Establishment, Physics Division, 21020 *Ispra* (*VA*), *Italy*

and A. Balerna and S. Mobilio

INFN – Laboratori Nazionali di Frascati, CP 13, 00044 *Frascati, Italy*

(*Received* 25 *November* 1986; *accepted* 3 *September* 1987)

Abstract

A laboratory dispersive mode spectrometer, capable of operating in either the analysing crystal transmission mode or a reflection mode, is described. Extended X-ray absorption fine structure (EXAFS) spectra of Re and ReO_2, obtained in the transmission mode, compare favourably with those from a scanning spectrometer at a synchrotron source. Factors affecting resolution, intensity and background in this transmission mode are discussed. Experiments with asymmetric reflection geometries, which have shown both improved resolution for X-ray absorption near edge structure (XANES) and reduced collection times, are reported. Methods of reducing backgrounds due to multiple Bragg reflections and Compton scattering are proposed.

Introduction

Extended X-ray absorption fine structure (EXAFS) is a powerful method for structural studies on a great variety of materials (Stern, Sayers & Lytle, 1975; Lee, Citrin, Eisenberger & Kincaid, 1981). The analysis of EXAFS spectra provides useful information for short-range-order studies because data can be obtained on interatomic distances, coordination numbers and disorder factors around a specific atom in a simple or complex matrix.

The best source for EXAFS studies is synchrotron radiation (SR) owing to its continuous spectrum and small beam divergence. Tunable monochromatic X-rays can be obtained with intensities several orders of magnitude higher than conventional laboratory sources. This implies shorter acquisition times, greater accuracy and the possibility of making measurements on dilute systems, biological samples and surfaces. However, the logistics of scheduling SR beam time at the few available facilities, travel and long waiting times are inconvenient. For this reason, there is interest in EXAFS laboratory facilities for studies which do not require high photon fluxes.

Laboratory facilities make use of the weak *Bremsstrahlung* spectrum from rotating anodes or conventional X-ray tubes. They work mainly in a scanning mode (Knapp, Chen & Klippert, 1978; Georgopoulous & Knapp, 1981; Khalid, Emrich, Dujari, Shultz & Katzer, 1981; Thulke, Haensel & Rabe, 1983; Cohen, Fischer, Colbert & Shevchik, 1980; Kampers, Duivenvoorden, van Zon, Brinkgreve, Viegers & Konigsberger, 1985). Monochromatic beams are produced by employing cylindrically curved crystals of the Johann or Johansson type in Rowland geometry. These methods give photon fluxes up to 10^7 counts s^{-1} at the sample.

For experiments requiring high resolution, a double-crystal monochromator in the $(+1+1)$ antiparallel geometry can be used, but with a great loss in the intensity of the incident beam (*i.e.* 300 counts s^{-1}). Recently, techniques have been developed in which the various energies, diffracted by an analysing crystal, diverge from a focus point and are dispersed in space. This divergent beam is intercepted at some distance from this point by a position-sensitive detector (PSD), giving a quasi-linear relation between energy and position.

The advantage of this method over the scanning technique is that the entire spectrum is obtained simultaneously without any mechanical motion. Long-term drifts in detectors are eliminated. The reduced collection time permits time-dependent studies.

While dispersive spectrometers were used or are under development at synchrotron facilities, their use in ordinary laboratories has been rare after the original work by Kaminaga, Matsushita & Kohra (1981). These latter authors show the EXAFS spectrum for Fe in the energy range of 7–8 keV with an

0021-8898/88/020079-07$03.00

estimated energy resolution of about 8 eV. An intensity of 10 counts s^{-1} above the absorption edge was available with a sealed-off X-ray tube and required a total counting time of 11 h with the sample in the beam. A reference normalization pattern without the sample required 4 h. Some Fe^{III} compounds were also measured with the same type of spectrometer (Nomura, Asakura, Kaminaga, Matsushita, Kohra & Kuroda, 1982).

A spectrometer suitable for dispersive EXAFS in both the transmission mode and the symmetric or asymmetric reflection mode was constructed and is described below.

Experimental arrangement

A. Transmission geometry

A diagram of the spectrometer in the transmission geometry is shown in Fig. 1. The arrangement for an asymmetrical reflection geometry, shown in Fig. 3, will be discussed later. The white beam from a sealed-off tungsten target X-ray tube has a 6° take-off angle which gives a 0·04 mm horizontal by 8 mm vertical effective source size. It diverges through a horizontal angle α as defined by scatter slits. It is diffracted by the (220) planes perpendicular to the surface of a thin (0·1 mm) Si crystal located on the axis and rotated by the θ drive of a $\theta,2\theta$ spectrometer. A relatively large source-to-crystal distance is required to reduce source angular divergence for the higher-resolution reflection mode. Since the divergent beam forms different Bragg angles with the (220) planes, different energies are diffracted at different points horizontally along the crystal. After transmission they are focused at a line (the image of the source) beyond the crystal, at a distance equal to the source-to-crystal distance (500 mm). A defining slit, placed at this focus, reduces background scattering due to Compton, multiple Bragg, air and slit-system scatter. Such a background reduction is important since the detector has no directional discrimination. The sample is placed just in front of this slit where the beam is very narrow. A position-sensitive detector with an active length of 40 mm is mounted 700 mm beyond the focus as shown. This distance represents a compromise between intensity, resolution and total energy range. The energy range is governed by the divergence angle α from the source or the crystal width if the beam extends beyond it. Similarly the active counter length may restrict the range.

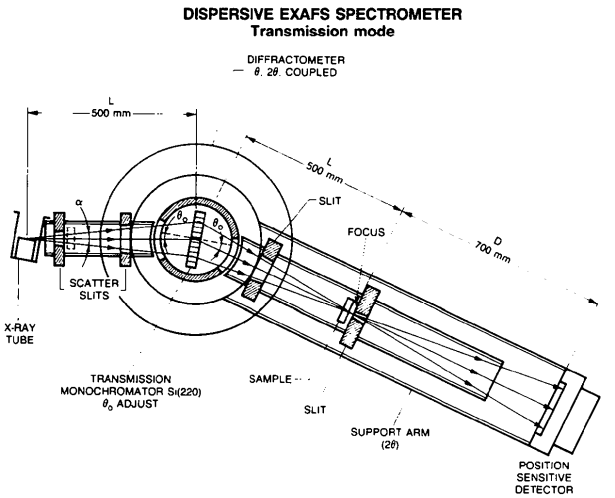

Fig. 1. Schematic view of the experimental apparatus. The diffracting crystal (transmission or reflection) is mounted on the θ angle drive while the sample and PSD are mounted on the 2θ drive of a standard X-ray diffractometer.

The photon energy range covered by the spectrometer can be changed by setting the central angle (θ_0 of Fig. 1) between the X-ray beam and the crystal planes, equal to the value given by the Bragg relation,

$$E_0 = hc/(2d \sin \theta_0), \tag{1}$$

where E_0 is the mean photon energy desired. The energy range covered depends on the geometrical acceptance of the crystal given by the equation

$$(E_{max} - E_{min})/E_0 = \alpha \cot \theta_0 \tag{2}$$

where E_{max} and E_{min} are the high- and low-energy limits and α is the angular width accepted by the crystal.

In order to obtain a good spatial resolution and a high counting rate, a high-pressure position-sensitive proportional counter (PSPC) was used. It has been shown (Broll, Henne & Krentz, undated) that an increase in the operating pressure improves the quantum efficiency and the spatial resolution of the position-sensitive detector. The latter is due to the shorter primary photoelectron range and to the possibility of using a higher voltage which allows better focusing of the cascading electrons. A xenon-filled PSPC, working at atmospheric pressure, can achieve a spatial resolution of about 150 μm and quantum efficiencies of 30% for Cu $K\alpha$ radiation. High-pressure PSPC's, using argon–methane gas mixtures, are capable of achieving ~60 μm spatial resolution and 50% quantum efficiencies for Cu $K\alpha$ radiation. Their quantum efficiency can reach 90% if xenon–methane is used. For this experiment a 40 mm long, 10 mm wide and 3 mm deep flow counter, filled with argon–methane gas, with an operating pressure of about 11 atm (1·14 MPa), was used at an operating voltage of 3·9 kV (the counter was purchased from Braun, Innovative Technology Inc., Munich, Federal Republic of Germany). The spatial resolution under these operating conditions was equal to about 100 μm. The energy resolution of the whole system is given by the relation

$$\Delta E/E_0 = [(s/D)^2 + (w/D)^2 + (r/D)^2 + \omega^2 + (\varphi^4/4) \tan^2 \theta_0]^{1/2} \cot \theta_0 \tag{3}$$

where s is the horizontal width of the X-ray source, r is the spatial resolution of the detector, ω is the intrinsic angular width of the dynamical crystal diffraction, φ is the vertical angular width accepted by the detector, $w = 2t \sin\theta_0$ (t being the crystal thickness) is the spatial broadening of the beam at the crystal due to the dynamical diffraction and thickness, and D is the distance from the focus to the counter. At first sight, the energy resolution expression (3) is similar to that of Kaminaga, Matsushita & Kohra (1981). However, it differs since the horizontal width of the X-ray source and the dynamical diffraction contribution depend on the focus-to-detector distance D and not on the source-to-crystal distance. Since the energy resolution does not depend on the source-to-crystal distance, this can be kept small to avoid intensity losses due to the vertical divergence of the beam. It is relatively large here for convenience in the reflection mode discussed later. The choice of D is a compromise between resolution and intensity. With the distances and the detector used in the present experimental set-up, the energy resolution was about 6 eV at 10 keV: the numerical value of (3) is $5{\cdot}3 \times 10^{-4}$ with the values and for the reflexion specified above, single contributions inside the square bracket of (3) being respectively 0·33, 0·85, 2·04, 0·09 and $0{\cdot}02 \times 10^{-8}$. Major contributions are, in order of importance, the spatial resolution of the detector, the crystal thickness and the X-ray source width. The total angular width accepted by the crystal ($\alpha = 50$ mrad) corresponds at 10 keV to an energy range $\sim 1{\cdot}5$ keV. The total intensity recorded was about 1600 counts s^{-1} over a useful range of 800 eV with the X-ray tube working at 20 kV (to avoid the presence of harmonics) and 30 mA. The intensity value is in good agreement with the expected total intensity estimated by taking into account the X-ray tube emissivity, the air absorption along the 1700 mm long X-ray path, the intensity of the dynamical diffraction by the crystal and the detector efficiency (about 30%) at 10 keV.

B. Reflection geometry

Before proceeding with the data analysis of this transmission dispersive method we consider some results of dispersive reflection modes. A dispersive reflection mode is shown in Fig. 2.

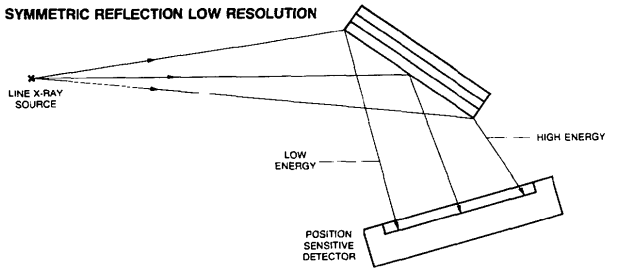

Fig. 2. Symmetric reflection mode.

Other researchers have used dispersive reflection spectrometers based on Si and LiF flat symmetrical crystals to obtain EXAFS spectra of solids and solutions (*e.g.* Taniguchi, Oka, Yamaki & Ikeda, 1980; Sano, Taniguchi & Yamatera, 1980; Sano, Maruo & Yamatera, 1983; Lossan, Neumann, Schlabitz & Wohlleben, 1987). These spectrometers were coupled with PSD's made of self-scanning photodiode arrays. The reflection mode has an advantage over the transmission mode in that the detector is closer to the source. In addition, with symmetric reflection one easily obtained crystal, with only one polished surface, covers all energy ranges. In contrast, the transmission mode requires crystals of small thickness with both surfaces polished, which are difficult to prepare. To improve the resolution over symmetric reflection, the asymmetric reflection arrangement of Fig. 3 was used (Maeda, Terauchi, Tanabe, Kamijo, Hida & Kawamura, 1982) with the advantage that a given energy range is spread out further in space. This reduces the effect of the PSD on the energy resolution. The asymmetric reflection also increases the reflected intensity by a factor $b^{1/2}$, $b = \sin(\theta + \alpha)/\sin(\theta - \alpha)$ being the asymmetry factor and α the angle between the crystallographic planes and the surface. In the present case b is greater than ten. The intensity increase is a consequence of the incident-beam Darwin acceptance width which is greater than the symmetric crystal acceptance width. The arrangement was originally set up to analyse a dilute solution of a uranium compound with an L_{III} edge at 17·2 keV. The 751 reflection of a standard 4 cm diameter (111) crystal gave a convenient asymmetric reflection with a total energy range of 250 eV. The energy resolution can be estimated by referring to (3). D is now the X-ray source-to-detector distance (~ 80 cm) and the effect of crystal thickness on resolution is replaced with the dynamical theory penetration depth. Since the effect of counter resolution is ten times less because of geometrical broadening, appreciable contributions are due to the source width and to the dynamical penetration depth. The value of $\cot\theta$ is reduced by a factor 2·15 and a

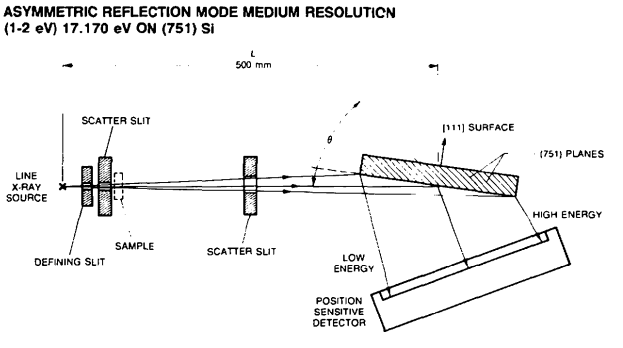

Fig. 3. Asymmetric mode. The spread-out exit beam reduces the PSD effect on resolution.

calculated energy resolution of less than 3 eV is obtained. Observations of the steepness of the L_{III} edge indicated 2–3 eV resolution.

Our experiments with this reflection mode revealed several problems with background that will require modification of the reflection method to obtain good EXAFS spectra. The background problem comes from Compton and air scattering. In normal well collimated diffraction geometries the background is negligible. Here, however, with no collimation between the crystal and the detector, the level of Compton and air scattering is high since the detector does not benefit from any directional discrimination. As a result, this scattering became comparable to or greater than the diffracted intensity of interest. Attempts to reduce this ratio by filtration, increasing the detector-to-crystal distance, or reducing the tube voltage only marginally improved this signal-to-background ratio. A more serious problem arose from what are commonly called 'glitches' in the spectrum of position (energy) *versus* intensity on the PSD display. Films at the detector position showed many reflections that are probably a mixture of Laue spots and multiple Bragg scattering of the type discussed by Renninger and others. For our short wavelengths there are one or more of these reflections every 1 or 2°. The films clearly showed that it was impossible to avoid all of these in the area of interest. Moving the detector 50 cm further from the crystal reduced the problem but again at the cost of decreased intensity. There are several possibilities for reducing the Compton and multiple-scattering problems. One method is to use double reflection of the $(n, -n)$ type. There are two ways of doing this. One is with a channel-cut monolithic crystal. This is difficult to construct with its flat polished internal surfaces and elastic hinge for harmonic suppression. The other way is to use two separate crystals. This requires sensitive and stable angle drives for alignment since the Darwin width for reflections of high Miller indices or for high energies can be as small as $\sim 0{\cdot}2''$ arc. In addition, some sort of active feedback control system would be required to maintain the two crystals in proper alignment.

Either of these crystal arrangements would almost completely suppress Compton or air-scatter background. Earlier it was believed that by having two separate crystals in this $(n, -n)$ 'channel-cut' arrangement the multiple-reflection 'glitches' could be removed by simply rotating one of the crystals about its reflecting plane. Recent experience with synchrotron monochromators (Dobson, Hasmain, Hart, van der Hoek & van Zuylen, 1987) shows that the number of 'glitches' increased after this rotation.

It seems then that dispersive EXAFS by reflection from a flat crystal would be difficult at the high energies (17·2 keV) attempted here. The main advantage of the transmission method, discussed earlier, is that it has a focus point and slits at this point which effectively eliminate background radiation at the counter and most of the Laue spots and 'glitches'. One of the important conclusions of this study is that a geometric arrangement involving a focus point and defining slits helps greatly in obtaining clean EXAFS spectra in the dispersive mode in the laboratory. A method of achieving this focusing by reflection has been set up at several synchrotron laboratories (Matsushita & Phizackerly, 1981; Flank, Fontaine, Jucha, Lemonnier, Raoux & Williams, 1983). White radiation from a distant (20 m) synchrotron source is incident on a triangular-shaped crystal bent in a cylindrical shape with a radius of ~ 10 m as shown in Fig. 4. The asymmetric reflection gives a focus point conveniently close to the crystal (30–40 cm) so that the PSD can be close to this focus point. To adapt this arrangement to a laboratory source requires a much shorter source-to-crystal distance ($P \sim 50$ cm) and a correspondingly smaller radius of curvature for the crystal ($R \sim 100$ cm) to obtain a crystal-to-focus distance q of ~ 20 cm. This smaller radius of curvature gives rise to greater problems of obtaining a sharp focus at point A in Fig. 4(*a*). A sharp focus is necessary

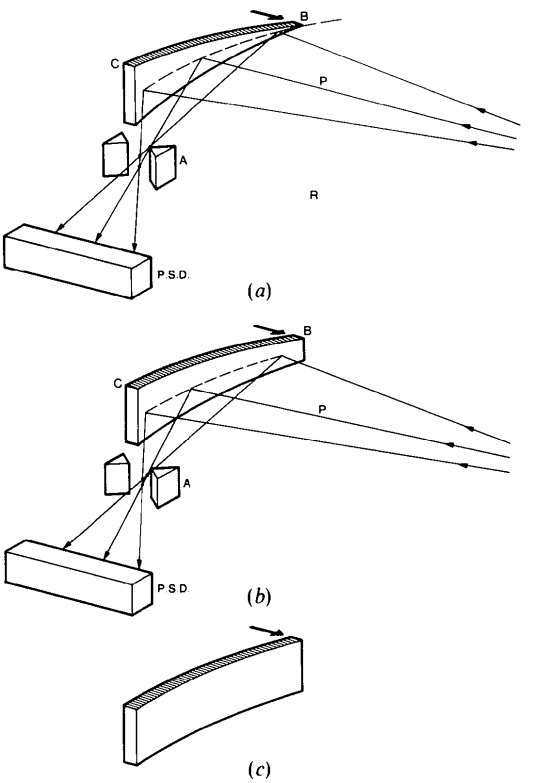

Fig. 4. Curved crystal reflection mode. In (*a*) bending the triangular crystal gives a constant radius of curvature from point *B* to *C*. The resulting extended focus at point *A* produces non-linearities on the energy scale at the PSD. 'Parabolizing' as in (*b*) or (*c*) gives a sharper focus and better linearity as shown in (*b*).

for good linearity (Suortti, Pattison & Weyrich, 1986). Graphic analysis or ray tracing shows that what is needed is not a constant radius of curvature as given by a triangular crystal but rather an increasing radius of curvature as one goes from point C to point B, a more 'parabolic' shape. This could be achieved by crystal shapes such as those of Fig. 4(*b*) or in a more pronounced form as shown in Fig. 4(*c*). The difficulty of getting the optimum shape under conditions where the Bragg angle and overall curvature are changed for different energy ranges makes it desirable to be able to vary these two parameters independently. A crystal holder with separate micrometer (and stepping-motor) controls for the overall bend and shape is currently under development. This holder is a modification of the one developed by other authors to obtain a logarithmic-spiral focusing monochromator (de Wolff, 1948; Webb, 1976). Although the shape problem is less severe for synchrotron arrangements, because of the large radius, it seems that they could also achieve better resolution with some crystal shaping.

Comparison of laboratory transmission dispersive EXAFS with synchrotron results

In this section a comparison is made between the spectra of the L_{III} edge of Re and ReO_2 obtained using the transmission laboratory system of Fig. 1 and the PULS EXAFS apparatus of the Frascati synchrotron radiation facility. The EXAFS spectra of the metal and of ReO_2 are shown in Figs. 5 and 6. The amplitudes

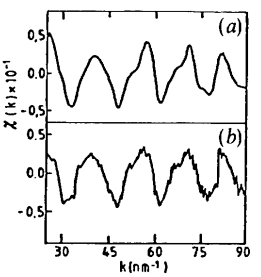

Fig. 5. EXAFS spectra of Re metal obtained using as X-ray source (*a*) synchrotron radiation and (*b*) a W X-ray tube.

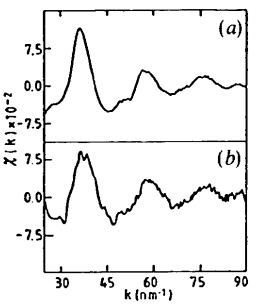

Fig. 6. EXAFS spectra of ReO_2 obtained using as X-ray source (*a*) synchrotron radiation and (*b*) a W X-ray tube.

and phases of these spectra are in good agreement. In order to evaluate the quality of our laboratory spectra, a complete EXAFS analysis was performed by Fourier transformation (FT) of the spectra and then by back transformation of the contributions due to the first coordination shell (Mobilio, Comin & Incoccia, 1982). In this way it was possible to obtain information on the mean coordination numbers (N), on the EXAFS Debye–Waller factors (σ^2) and on the nearest-neighbour distances (R_{nn}). In fact, the inverse Fourier transform allows one to analyse separately the amplitude function, $A(k)$, and the 'total' phase factor $\pi(k)$. $A(k)$ is related to N and σ^2 by the following equation:

$$A(k) = (S_0^2 N/kR_{nn}^2) \exp(-2k^2\sigma^2)|f(k,\pi)|$$

where $|f(k,\pi)|$ is the backscattering amplitude of the neighbouring atoms and S_0^2 is the reduction factor due to multielectron excitations. The 'total' phase factor, given by

$$\pi(k) = 2kR_{nn} + \varphi_{L_{III}},$$

is related to the nearest-neighbour distance and $\varphi_{L_{III}}$ represents the k-dependent phase shift for d-symmetry final states. In order to use these equations, one must know the scattering functions $|f(k,\pi)|$ and $\varphi_{L_{III}}$. It is known (Citrin, Eisenberger & Kincaid, 1976) that such functions can be transferred from one system to another but, particularly for $|f(k,\pi)|$, this is possible only if the two systems are chemically similar (Stern, Bunker & Heald, 1980).

For these reasons we used as a reference the $|f(k,\pi)|$ and $\varphi_{L_{III}}$ derived by back transformation of the first FT peak of the synchrotron radiation spectra of Re and ReO_2. If one plots the function

$$\ln[A(k)_{lab}/A(k)_{synch}]$$

against k^2, a straight line must be obtained, whose slope and extrapolated value for $k^2 = 0$ are

$$-2[(\sigma_{lab})^2 - (\sigma_{synch})^2]$$

and

$$\ln[(N/R^2)_{lab}/(N/R^2)_{synch}],$$

respectively.

It is also possible to compare the nm^{-1} distances in k space (Figs. 5*b* and 6*b*) with the relation

$$R_{lab} - R_{synch} = [\pi_{lab}(k) - \pi_{synch}(k)]/2k.$$

Figs. 7 and 8 show the results of an experimental comparison of Re spectra obtained in the laboratory using the described apparatus with a synchrotron radiation spectrum for Re and ReO_2, respectively. A quite linear behaviour is obtained, as expected. A linear fit to such straight lines allows calculation of the structural parameters R, N and σ^2.

As shown in Table 1, the values relative to the laboratory measurements are in good agreement with

Table 1. *Comparison between laboratory and synchrotron radiation results*

The difference between the values of the nearest-neighbour distances, the ratio between the mean values of the coordination numbers and the difference between the EXAFS Debye–Waller factors are reported in the second, third and fourth columns respectively.

Sample	ΔR_{nn} (nm)	N_{lab}/N_{synch}	$\Delta\sigma$ (nm^2)
Re	2×10^{-3}	0·96	$-0{\cdot}21 \times 10^{-5}$
ReO_2	2×10^{-3}	0·95	$-0{\cdot}26 \times 10^{-5}$

the synchrotron radiation values: the small differences can be attributed to the different signal-to-noise ratio between the compared EXAFS spectra.

Concluding remarks

The EXAFS results obtained in this work show that a simple laboratory spectrometer involving the dispersive transmission mode can be used whenever long collection times (10–20 h) and moderate resolution (5–10 eV) can be tolerated. The spectra of Re and ReO_2 compare well with those obtained at a synchrotron radiation facility.

Flat-plane symmetric and asymmetric reflection geometries, particularly the latter, offer advantages in increased intensity and resolution as well as greater ease in crystal fabrication compared with the transmission geometry. However, they suffer from a high Compton background and various 'glitches' because they lack a focus point and defining slits. It would seem that the most flexible system for laboratory EXAFS in the dispersive mode would be a curved-crystal arrangement of the type employed at some synchrotron sources but suitably modified to give the required crystal bending and shaping to accommodate the shorter X-ray source-to-crystal distances. In addition a PSD made of a photodiode array would have greater efficiency, with shorter collection times (by a factor of ~ 5) and with greater spatial resolution than a PSPC.

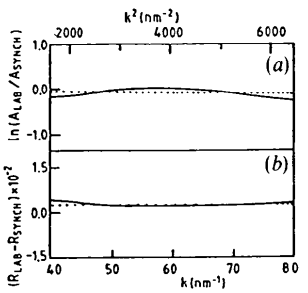

Fig. 7. (*a*) Plot of $\ln[A(k)_{lab}/A(k)_{synch}]$ *versus* k^2 and (*b*) plot of $\Delta(R_{lab} - R_{synch})$ (nm) *versus* k for Re. Full line: experimental behaviour; dotted line: linear fit to the experimental behaviour.

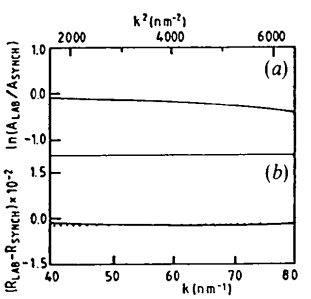

Fig. 8. (*a*) Plot of $\ln[A(k)_{lab}/A(k)_{synch}]$ *versus* k^2 and (*b*) plot of $\Delta(R_{lab} - R_{synch})$ (nm) *versus* k for ReO_2. Full line: experimental behaviour; dotted line: linear fit to the experimental behaviour.

The authors are grateful to Professor M. Calamiotou, University of Athens, for calculations, to Dr D. D'Adamo for his help in computer data collection, and to Mr D. Inzaghi for his technical assistance.

References

BROLL, N., HENNE, M. & KRENTZ, W. (Undated). *Siemens Analytical Application Notes*, No. 271. Siemens Analytical Instruments, New Jersey, USA.

CITRIN, P. H., EISENBERGER, P. & KINCAID, B. M. (1976). *Phys. Rev. Lett.* **36**, 1346–1349.

COHEN, G. G., FISCHER, D. A., COLBERT, J. & SHEVCHIK, N. J. (1980). *Rev. Sci. Instrum.* **51**, 273–277.

DOBSON, B. R., HASMAIN, S. S., HART, M., VAN DER HOEK, M. J. & VAN ZUYLEN, P. (1987). *J. Phys. (Paris)*. In the press.

FLANK, A. M., FONTAINE, A., JUCHA, A., LEMONNIER, M., RAOUX, D. & WILLIAMS, C. (1983). *Nucl. Instrum. Methods*, **208**, 651–654.

GEORGOPOULOS, P. & KNAPP, G. S. (1981). *J. Appl. Cryst.* **14**, 3–7.

KAMINAGA, U., MATSUSHITA, T. & KOHRA, K. (1981). *Jpn. J. Appl. Phys.* **20**, L355–L358.

KAMPERS, F. W. H., DUIVENVOORDEN, F. B. M., VAN ZON, J. B. A. D., BRINKGREVE, P., VIEGERS, M. P. A. & KONIGSBERGER, D. C. (1985). *Solid State Ionics (Netherlands)*, **16**, 55–63.

KHALID, S., EMRICH, R., DUJARI, R., SHULTZ, J. & KATZER, J. R. (1981). *Rev. Sci. Instrum.* **53**, 22–33.

KNAPP, G. S., CHEN, H. & KLIPPERT, T. E. (1978). *Rev. Sci. Instrum.* **49**, 1658–1666.

LEE, P. A., CITRIN, P. H., EISENBERGER, P. & KINCAID, B. (1981). *Rev. Mod. Phys.* **53**, 769–806.

LOSSAN, N., NEUMANN, G., SCHLABITZ, W. & WOHLLEBEN, D. (1987). Abstract of the 7th General Conference of the Condensed Matter Division of the EPS, Pisa, Italy, p. 129; and private communication.

MAEDA, H., TERAUCHI, H., TANABE, K., KAMIJO, N., HIDA, M. & KAWAMURA, H. (1982). *Jpn. J. Appl. Phys.* **21**, 1342–1346.

MATSUSHITA, T. & PHIZACKERLY, R. P. (1981). *Jpn. J. Appl. Phys.* **20**, 2223–2228.

MOBILIO, S., COMIN, F. & INCOCCIA, L. (1982). Internal Report No. 83/19 (NT). Lab. Naz. di Frascati, Italy.

NOMURA, M., ASAKURA, K., KAMINAGA, U., MATSUSHITA, T., KOHRA, K. & KURODA, H. (1982). *Bull. Chem. Soc. Jpn*, **55**, 3911–3914.

SANO, M., MARUO, T. & YAMATERA, H. (1983). *Chem. Phys. Lett.* **101**, 211–214.

SANO, M., TANIGUCHI, K. & YAMATERA, H. (1980). *Chem. Lett.* pp. 1285–1286.

STERN, E. A., BUNKER, B. A. & HEALD, S. M. (1980). *Phys. Rev. B*, **21**, 5521–5539.

STERN, E. A., SAYERS, D. E. & LYTLE, F. W. (1975). *Phys. Rev. B*, **11**, 4836–4846.

SUORTTI, P., PATTISON, P. & WEYRICH, W. (1986). *J. Appl. Cryst.* **19**, 336–342.

TANIGUCHI, K., OKA, K., YAMAKI, N. & IKEDA, S. (1980). *Advances in X-ray Analysis*, Vol. 24, pp. 117–180. New York: Plenum Press.

THULKE, W., HAENSEL, R. & RABE, P. (1983). *Rev. Sci. Instrum.* **54**, 277–283.

WEBB, N. G. (1976). *Rev. Sci. Instrum.* **47**, 545–547.

WOLFF, P. M. DE (1948). *Appl. Sci. Res. B*, **1**, 119–126.